Title

Early-childhood social reticence predicts SCR-BOLD coupling during fear extinction recall in preadolescent youth.

Authors

Michalska, KJ
Feldman, JS
Ivie, EJ
et al.

Publication Date

2019-04-01

DOI

10.1016/j.dcn.2018.12.003

Peer reviewed

Developmental Cognitive Neuroscience 36 (2019) 100605

Contents lists available at ScienceDirect

Developmental Cognitive Neuroscience

journal homepage: www.elsevier.com/locate/dcn

Early-childhood social reticence predicts SCR-BOLD coupling during fear extinction recall in preadolescent youth

K.J. Michalska[a,*], J.S. Feldman[b], E.J. Ivie[c], T. Shechner[d], S. Sequeira[b], B. Averbeck[e], K.A. Degnan[f], A. Chronis-Tuscano[g], E. Leibenluft[e], N.A. Fox[h], D.S. Pine[e]

[a] University of California Riverside, Department of Psychology, Riverside, CA, USA
[b] University of Pittsburgh, Department of Psychology, Pittsburgh, PA, USA
[c] University of Oregon, Department of Psychology, Eugene, OR, USA
[d] University of Haifa, Department of Psychology, Haifa, Israel
[e] The National Institute of Mental Health, Emotion and Development Branch, Bethesda, MD, USA
[f] The Catholic University of America, Department of Psychology, Washington D.C., USA
[g] University of Maryland College Park, Department of Psychology, College Park, MD, USA
[h] University of Maryland College Park, Department of Human Development and Quantitative Methodology, College Park, MD, USA

ARTICLE INFO

Keywords:
Temperament
Conditioning
Extinction recall
fMRI
Skin conductance response
Coupling

ABSTRACT

Social Reticence (SR) is a temperament construct identified in early childhood that is expressed as shy, anxiously avoidant behavior and, particularly when stable, robustly associated with risk for anxiety disorders. Threat circuit function may develop differently for children high on SR than low on SR. We compared brain function and behavior during extinction recall in a sample of 11-to-15-year-old children characterized in early childhood on a continuum of SR. Three weeks after undergoing fear conditioning and extinction, participants completed a functional magnetic resonance imaging extinction recall task assessing memory and threat differentiation for conditioned stimuli. Whereas self-report and psychophysiological measures of differential conditioning, extinction, and extinction recall were largely similar across participants, SR-related differences in brain function emerged during extinction recall. Specifically, childhood SR was associated with a distinct pattern of hemodynamic-autonomic covariation in the brain when recalling extinguished threat and safety cues. SR and attention focus impacted associations between trial-by-trial variation in autonomic responding and in brain activation. These interactions occurred in three main brain areas: the anterior insular cortex (AIC), the anterior subdivision of the medial cingulate cortex (aMCC), and the dorsolateral prefrontal cortex (dlPFC). This pattern of SCR-BOLD coupling may reflect selective difficulty tracking safety in a temperamentally at-risk population.

1. Introduction

Encountering threats evokes a cascade of autonomic changes. These include reflexive skin conductance responses (SCRs, Boucsein, 1992; Dawson, Schell & Filion, 2007), which interact with the brain dynamically to optimize behavior (Nieuwenhuis et al., 2011). Dynamic interactions between SCRs and the brain may unfold differently in children with different temperamental profiles, such as high vs. low levels of social reticence or shyness. While prior functional magnetic resonance imaging (fMRI) studies examine threat circuit function in such children (Britton et al., 2013; Shechner et al., 2018), none examine associations among temperament, SCRs, and neural responses to threats. Here, we relate individual differences in early emerging, longitudinally assessed, socially reticent behavior to interactions between moment-to-moment brain activity and SCRs during a fear extinction recall paradigm.

Responding appropriately to threats relies in part on our capacity to learn subtle threat–safety discriminations. Research on fear conditioning generates insights on how such learning occurs. During fear conditioning, a neutral stimulus (conditioned stimulus, CS+) is paired with an aversive stimulus (unconditioned stimulus, UCS) until a CS+-threat association is formed. In extinction, the CS + is presented in the absence of the aversive UCS, resulting in a new CS+-safe association. The CS- is never paired with the UCS. Extinction recall then occurs when, at a later time, the extinguished CS + is presented again. Thus, extinction recall, the retention of extinction learning over time, quantifies one form of threat-safety discrimination. Yet work on the mechanisms mediating extinction recall in children remains limited. Given

* Corresponding author.
E-mail address: kalina.michalska@ucr.edu (K.J. Michalska).

https://doi.org/10.1016/j.dcn.2018.12.003
Received 3 May 2018; Received in revised form 16 November 2018; Accepted 11 December 2018
Available online 12 December 2018

evidence of developmental changes in extinction recall capacity (Michalska et al., 2016), more research is needed.

Prior research sets the stage for studies that specifically examine associations among temperament, SCR, and the neural mechanisms mediating extinction recall. A recent fMRI study suggests that dysregulation of the neural mechanisms underlying extinction recall may confer vulnerability for anxiety in temperamentally inhibited individuals (Shechner et al., 2018). This study compared neural responding during extinction recall in adults who had manifested different degrees of longitudinally assessed early-childhood inhibited temperament. Threat-safety discrimination was examined using morphs that combined features of the extinguished CS + and CS- cues (i.e., generalization stimuli, GS). Two weeks following fear conditioning and extinction, participants appraised CSs and GSs during extinction recall. In this task, childhood inhibited temperament was associated with greater activation in subgenual anterior cingulate cortex (ACC) in response to cues signaling safety, potentially reflecting neural correlates that promote resilience against anxiety in a temperamentally at-risk population.

Shechner et al. (2018) only examined brain function in adulthood, specifically in response to potential threat cues, independent of physiological parameters, such as SCR. Because an individual neural circuit influences multiple physiological processes, prior imaging studies have been designed to elucidate pathophysiology by comparing circuitry-physiology coupling in health and disease. For example, in bipolar disorder, this approach has been used to study attention-related fluctuations quantified in reaction time (Pagliaccio et al.,2017), whereas in autism, it has been used to examine social processes associated with eye gaze (Dalton et al., 2005). For anxiety-related states, preliminary work used a related approach in adults to examine associations between SCR and engagement of threat-responsive brain circuitry (Knight et al., 2005). Similar to studies in bipolar disorder and autism, this prior work suggested that measures of dynamic interactions between SCR and neural responses may detect stronger associations between anxiety-related states and brain function than do overall measures of brain function. Specifically, the work found threats to induce heightened coupling between SCR and activity in threat-responsive neural circuitry. Given prior findings on engagement of threat-responsive circuitry in anxiety to either safe or ambiguous cues (Shechner et al., 2018; Lissek et al., 2010), one would expect levels of anxiety related traits in the current study to positively correlate with levels of SCR-brain activity coupling to either neutral or ambiguous stimuli.

The current study extends Shechner et al. (2018) by examining levels of such SCR-brain activity coupling in children assessed longitudinally for levels of social reticence (SR). We focus on SR, which is expressed as shy, anxiously avoidant behavior to a novel peer across childhood (Degnan et al., 2014). SR is conceptually similar to infant and toddler assessed behavioral inhibition (BI) in that the two constructs are thought to represent developmentally relevant expressions of fearfulness in the face of unfamiliarity. While BI encompasses behavioral reactions to both unfamiliar objects or challenging social situations, the hallmark of SR is socially wary behavior in the company of unfamiliar peers (Rubin et al., 2018). In this respect, SR is considered equivalent to the construct of social inhibition (e.g., Kochanska & Radke-Yarrow, 1992; Rubin et al., 2002). Moreover, SR typically refers to behaviors manifested at later ages than the behaviors typically rated in assessments of BI. Several reports document that high levels of socially reticent behavior are associated with the inability to regulate negative emotions, thus potentially placing children with SR at risk for developing anxiety disorders (Rubin et al., 2009; Rubin and Burgess, 2001).

Brain imaging studies have examined threat-evoked autonomic reactions in healthy adults. Such studies typically employ paradigms that present participants with threatening stimuli, assess changes in peripheral physiology, and model dynamic relationships between physiology and brain response (e.g. Eisenbarth et al., 2016; Knight et al., 2005). SCR, an autonomic arousal measure of the sympathetic nervous system, is a sensitive measure of peripheral physiological reactivity that is directly influenced by cortical and subcortical brain regions. Regions associated with SCR to threat include the cingulate cortex, insular cortex, amygdala, and orbitofrontal and medial prefrontal cortices (Büchel et al., 1998; Critchley et al., 2000, 2011; Critchley and Harrison, 2013; Fredrickson et al., 1998; Nagai et al., 2004; Phelps et al., 2001; Tranel & Damasio, 1994; Williams et al., 2001, 2005). To our knowledge, no such study examines children, and none examine relationships among simultaneous SCR-brain responses and individual differences in temperament at any age. If we are to fully appreciate linkages across autonomic, neural, and experiential systems, this sort of multimethod approach is essential.

The current study uses a recently-developed paradigm (Michalska et al., 2016) to examine brain activity related to SCRs during fear extinction recall in 11-to-15-year-old children falling along a continuum of social reticence assessed in toddlerhood and early childhood. We collected fMRI, SCR, and self-report data to test two hypotheses. First, based on work in adults, we expected SCR-related associations to be present in brain regions involved in interoception and autonomic regulation (e.g. insula, anterior cingulate cortex, prefrontal cortex). Second, we tested the hypothesis that the pattern of covariation between central and peripheral response systems (i.e., between brain activation and SCRs) would be different for children high on longitudinally-assessed SR than children low on SR. Finding such differential patterns would isolate aspects of brain function related to SR that manifest with a large effect size. By successfully isolating these relations, such effect sizes would be greater than the simpler relationships between levels of SR and overall brain function, independent of covariation with SCR. Of note, heightened threat responsivity has previously been associated with increased SCR-fMRI coupling (Knight et al., 2005). Moreover, prior work finds perturbed neural and autonomic responses in anxiety specifically to ambiguous threats or safety cues, as opposed to conditioned threat cues (Kaczkurkin et al., 2016; Lissek et al., 2010, 2014). As a result, in the current study, we expected to detect some form of heightened SCR-fMRI covariation in children high on social reticence, particularly in response to either ambiguous threat or safety cues. However, such hypotheses remain relatively broad, given the lack of empirical work on SCR-fMRI coupling among children, including temperamentally reticent children.

2. Methods and materials

2.1. Participants

Participants were recruited from the community at 2 years of age and enrolled in an ongoing longitudinal study. Individuals in this unselected sample served as age- and gender-matched comparisons for another sample targeted in the longitudinal study (Jarcho et al., 2016). Those in this second sample were recruited as infants and enrolled on the basis of their expression of behaviorally inhibited temperament. This second sample did not complete the current study. As part of this larger study, children were assessed on SR using maternal report questionnaires and behavioral observations collected at 2, 3, 4, 5, and 7 years. At 11 years, participants were eligible for the current study if they were medication free, not color blind, had an IQ > 70, and reported no contraindications for neuroimaging. Participants also had to be free from psychopathology requiring immediate treatment, meaning a need for treatment currently, within the next few weeks, based on the assessment of a trained clinician. Such a need reflected the presence of significant ongoing symptoms of suicidal ideation, psychosis or pervasive developmental disorder, that are of sufficient severity to cause significant functional impairment, for which the research participant is not receiving treatment. This judgement was made by the trained clinician performing the clinical assessment, in consultation with DSP and ACT. Participants who verbally assented and whose primary

caregivers gave written consent were enrolled. Procedures were approved by the University of Maryland, College Park and the National Institute of Mental Health (NIMH) Institutional Review Boards. The paradigm consisted of two visits. Visit 1 included the fear conditioning and extinction phase. Visit 2 included the extinction recall phase. For each visit, families were compensated for their time.

2.2. Social reticence

As part of a larger study, participants were assessed on SR using maternal report questionnaires and behavioral observations collected at 2, 3, 4, 5, and 7 years of age. As in the study by Jarcho et al. (2016), a composite SR score was computed from the 24 & 36-month Social Fear subscale from the Toddler Behavioral Assessment Questionnaire (Goldsmith, 1996), the 48-month, 60-month and 7-year Shyness subscale from the Children's Behavior Questionnaire (CBQ), a maternal report of children's shyness (Rothbart et al., 2001), and measures of the child's socially reticent behavior during standardized laboratory interactions with unfamiliar, age-matched peers at 2, 3, 4, 5, and 7 years of age. The alpha reliability across these measures is .80. Full details of how the SR behavior was observed and coded are provided in Degnan et al. (2011, 2014). In brief, children interacted with an unfamiliar peer in the laboratory during identical *free play*, *cleanup* and *social problem-solving* episodes at each age. For the *free play* episode, a range of age appropriate toys were scattered across the floor, and children were allowed to play for 10 min. Behavior was rated for wariness and unfocused/unoccupied behavior. Wariness was defined as a hesitancy to play with the toys and included behaviors such as hovering, watching, and self-soothing. Unfocused/ unoccupied behavior was defined as time spent disengaged from any activity. For the *cleanup* episode, children were instructed to clean up the toys and were left for a maximum of 5 min to clean up together. Coders assessed the duration of time spent cleaning up the toys, refusing to clean up the toys, and unoccupied in either play or cleanup behavior. Lastly, for the *social problem-solving* episode, children were asked to share a developmentally appropriate toy typically designed for one child's use. The experimenter entered the room with the special toy, told the children they only had one special toy so they must share and take turns, and then left the room for 5 min. Social initiations were coded based on schemes used by Rubin and Krasnor (1983) and Stewart and Rubin (1995). Social wariness from free play, proportion of time unoccupied/onlooking from cleanup, and proportions of passive strategies used in social problem-solving were standardized and averaged to represent SR behavior at each age. All parent-report and behavior scores were standardized within time-point and averaged together. This composite measure of overall SR was utilized because combining data from different activities, informants, and ages better reflects behavioral tendencies than a single measure at one time-point. Higher composite scores indicate higher levels of childhood SR.

A total of 62 children between the ages of 11 and 15 years participated in the fear conditioning and extinction procedures. One child discontinued participation because of anxiety during fear acquisition, and two were excluded due to color blindness, leaving 59 children who contributed data. The second visit, 3 weeks later, included an extinction recall task during fMRI scanning. Some participants were unable to complete the second visit due to scheduling conflicts (n = 2), equipment failure (n = 1), or dental braces (n = 6). Thus, 50 children participated in extinction recall procedures. Of these 50 children, one child discontinued participation when they became anxious, two were excluded due to missing SR data, and 4 were excluded from fMRI analyses due to excessive motion (see Data Analysis). Therefore 43 participants were included in the final sample for Visit 2 of the study. SCR data from 6 participants were not usable at extinction recall due to equipment failure; however, these participants did provide usable SCR data at conditioning and imaging data at extinction recall and were thus retained. Demographics are presented in Table 1.

2.3. Visit 1: fear conditioning task

Participants underwent a developmentally-appropriate differential fear conditioning paradigm used previously (Michalska et al., 2016; Shechner et al., 2015) (Fig. 1). Fear conditioning consisted of a *pre-acquisition* and an *acquisition* phase. In *pre-acquisition*, children viewed one blue and one yellow cartoon bell, the CS, in the absence of the UCS. During *acquisition*, one bell, the CS+, predicted the UCS, an unpleasant, loud alarm sound, presented at 95 dB for 1 s concurrently with a red bell figure, while the other bell, the CS-, did not. The CS + was followed by the UCS with an 80% reinforcement schedule. The CS + and CS- assignment was counterbalanced across participants. Participants were told that they could learn to predict when the UCS would occur, but they were not explicitly informed of the CS/UCS contingency. During fear extinction, the CS + and CS- were presented repeatedly in the absence of the UCS. During pre-acquisition, both the CS + and CS- were presented for 8 s. During acquisition, the CS- and non-reinforced CS+ (2 trials) were presented for 8 s, and the reinforced CS+ (8 trials) was presented for 7 s, followed by a red bell for 1 s. CS + and CS- were presented for 8 s during extinction. All CS + and CS- were followed by an inter-stimulus interval (ISI) of a blank gray screen presented for 8–21 seconds (mean = 15 s).

SCR to the CSs was recorded from two Ag/AgCl electrodes from the medial phalanx of the middle and ring fingers of the non-dominant hand with a PsyLab psychophysiological recording system (PsyLab SAM System Contact Precision Instruments, London, www.psylab.com) using a sampling rate of 1000 Hz. Following each of the three phases, children also completed subjective fear ratings to the CS + and CS- using a 10-point Likert scale (1 = none to 10 = extreme).

2.4. Visit 2: in-scanner extinction recall task

Three weeks after fear conditioning and extinction (mean = 22.74 ± 8.28 days), participants underwent MRI scanning during an *extinction recall* task (adapted from Michalska et al., 2016). At this visit, participants viewed the CS + and CS- and four morphed images consisting of different blends of the CS- and CS+ (CS-, 20% CS+, 40% CS+, 60% CS+, 80% CS+, 100% CS+) (Fig. 1). The stimulus array at extinction recall was designed to capture the transitional boundary between perceived threat and safety using morphed images (Lissek et al., 2009, 2010) and to measure behavioral, autonomic, and neural response gradients along a continuum. In two runs of 72 trials each, six blocks of each task instruction (threat appraisal, explicit memory) per run were presented in random order. These reiterations resulted in 12 presentations of each morph for each task instruction (threat appraisal, explicit memory). Blocks were composed of 12 morphs presented randomly for 4000 ms with a 200–10000 ms inter-stimulus interval (mean 5 s). Participants used a slider button box to answer one of two questions on a scale from 0 to 6 in response to each bell: 1) How afraid are you of this bell now? (threat appraisal); 2) How likely was the bell to ring in the past? (explicit memory). SCR was obtained from the index and middle fingers of the non-dominant hand using an MRI-compatible MP-150 system (BIOPAC Systems, Inc., CA, USA) at a sampling rate of 1000 Hz. The task was programed in E-prime (PST Inc., Pittsburgh, PA).

2.5. Visit 1 SCR and behavioral data analysis

SCR to each CS + and CS- was determined by the difference between peak amplitude (within 1–5 seconds following stimulus onset) and baseline activity (minimum amplitude within 0–1 s prior to stimulus onset). The SCR data were square-root transformed and averaged across all trials in each condition. Repeated measures ANOVA with Phase (pre-conditioning, conditioning, extinction) and Stimulus type (CS+, CS-) as within-subject factors and SR as continuous between group covariate, was used to examine main effects and interactions of SR. Similar analyses were used to examine self-report measures

Table 1
Demographic characteristics of the children in the analyses.

	N					Race/ethnicity				
Task and Measure	Total	Female (%)	Age in years (M, SD)	IQ (M, SD)	Social Reticence (M, SD)	Hispanic (%)	Caucasian (%)	African-American (%)	Asian (%)	Other (%)
			Fear acquisition and extinction							
Self-report	59	44.1%	13.35 (0.63)	113.46 (20.03)	0.08 (0.58)	5.1%	61.0%	22.0%	1.7%	15.4%
SCR	55	40.0%	13.32 (0.64)	113.44 (20.46)	0.10 (0.57)	5.5%	61.8%	21.8%	0.0%	16.3%
			Extinction recall							
With SCR	37	40.5%	13.33 (0.63)	117.22 (12.88)	0.09 (0.62)	5.4%	59.5%	24.3%	0.0%	16.2%
Without SCR	43	44.2%	13.38 (0.62)	116.37 (12.99)	0.09 (0.63)	4.7%	55.8%	25.6%	2.3%	16.3%

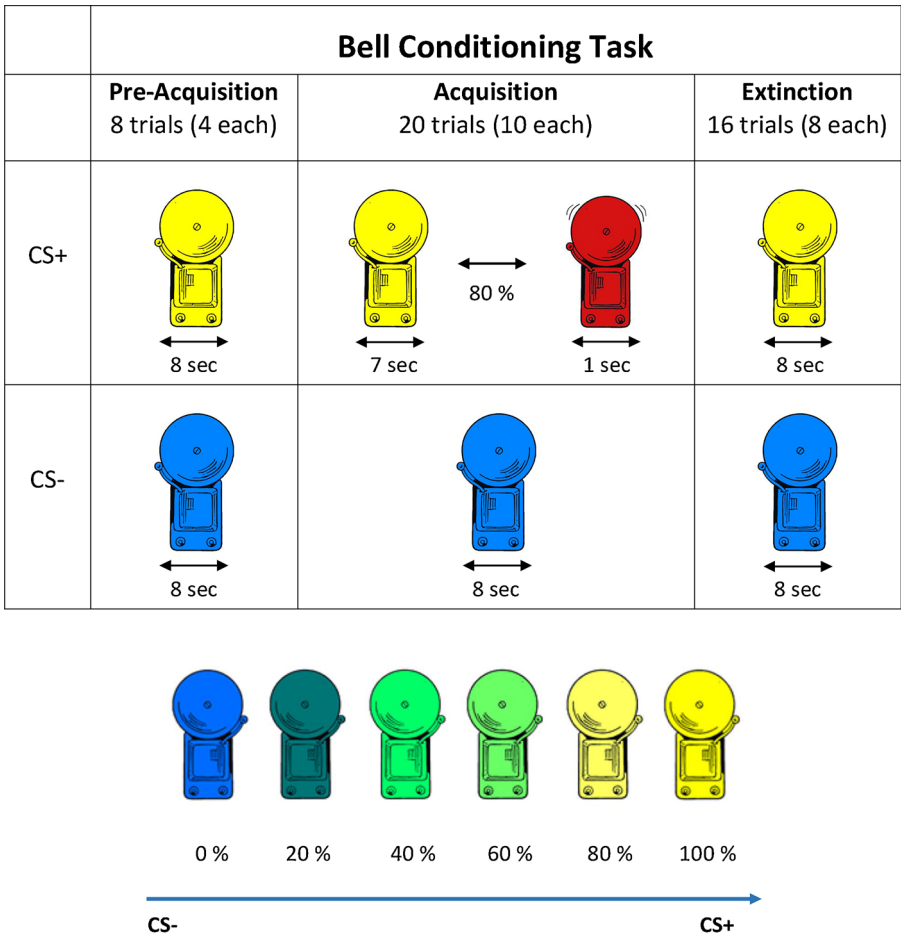

Fig. 1. A schematic depiction of A. the preacquisition, acquisition, and extinction phases of the conditioning paradigm and B. the generalization stimuli during the extinction recall task. CS = conditioned stimulus.

obtained prior to and immediately after fear conditioning, and immediately after fear extinction.[1] All statistical analyses were performed using SPSS software and statistical significance was set to $\alpha < 0.05$.

A reinforcement-learning model was fit to the SCR of each subject on a trial-by-trial basis, as in Michalska et al. (2017) (see also Costa et al., 2016; Li et al., 2011 for a similar approach). The model updates the predicted SCR, v, of the CS + using the response to the UCS, r, in trial t as follows:

$$v(t) = v_i(t-1) + \alpha(r(t) - v_i(t-1))$$

Thus, the updated predicted SCR of the CS + is given by its value during the immediately preceding trial, $v_i(t-1)$ plus a change based on the difference between the actual response to the UCS and the predicted response $(r(t) - v_i(t-1))$, multiplied by the learning rate parameter (α). At the beginning of each conditioning phase the value, v, of the CS + was set to 0. The learning rate parameter α was fit by minimizing the sum of squares between the measured SCR and the model's prediction of the SCR. Statistical significance was set to $\alpha = 0.05$.

[1] EMG data were collected but were not the focus of the current paper and are not discussed.

2.6. Visit 2 imaging acquisition and analysis

Neuroimaging data were collected using a 3 T General Electric 750 scanner and 32-channel head coil. During 2 runs of 13 min 9 s each, 343 functional image volumes, with 47 contiguous interleaved axial slices (in-plane resolution 2.5 mm, 3 mm slice thickness) were obtained with a T2*-weighted echo-planar sequence (TR = 2300 ms; TE = 25 ms; flip angle = 50; Field of View (FOV) = 240 mm; matrix = 96 × 96). Functional data were anatomically localized and coregistered to a high-resolution T1-weighted volumetric scan of the whole brain, using a magnetization prepared gradient echo sequence (MPRAGE) [TE = min full; TI = 425 ms; flip angle = 7; FOV = 256 mm; matrix = 256 × 256; in plane resolution 1.0 mm].

Imaging data were analyzed using AFNI (Analysis of Functional NeuroImages [http://afni.nimh.nih.gov/afni/]) with standard preprocessing. Individual preprocessing of echo-planar data included slicetime correction, motion correction, spatial normalization to the MNI template, and spatial smoothing with a 6 mm full-width half-maximum (FWHM) kernel. BOLD data were scaled at the voxel-wise time series by their temporal means so that the effect estimates could be interpreted as percent signal change relative to the mean.

To control for head motion and based on our previous work with pediatric populations (Britton et al., 2013; Shechner et al., 2018), we excluded pairs of successive TRs where the relative head displacement exceeded 2 mm. We also excluded time points where more than 10% of the masked brain voxels were outliers. Time points were excluded via censoring in the linear regression. Total head motion index was not correlated with SR ($p = .661$).

SCR for each CS and GS was determined by the difference between baseline-to-peak amplitude within 5 s after stimulus onset, as is the standard approach both in our studies (Michalska et al., 2017) and other studies (Balderston & Helmstetter, 2010). Baseline was determined as minimum amplitude within 0–1 s prior to stimulus onset. Peak amplitude was determined as the maximum value within 1–5 seconds following stimulus onset. Peak values for each trial were normalized to that trial's baseline SCR and expressed as a percent change from that baseline value (Michalska et al., 2017; Balderston & Helmstetter, 2010). Outliers were determined by computing the global SCR average (across all trials) for each participant. Individual trials that fell above or below 3SD of the global average were regarded as artifacts and replaced with that participant's global average.

For each participant, a general linear model included 12 condition regressors (6 regressors for each morph in each of the two attention states). Third-order Legendere polynomials modeling baseline drift and 6 head motion parameters were also included to control for potential confounding effects. This allowed us to examine average stimulus-locked BOLD responses, as in standard fMRI analyses. A second model included regressors for modulation by SCR on CS+, CS-, and morph trials. Including amplitude modulation by trial-wise SCR allowed us to examine trial-by-trial associations between variation in BOLD response and variation in SCR. Regression coefficients for the amplitude modulation effects indicate differences in percent signal change per micromho (μmho) increase above one's mean SCR, indexing the strength of the SCR-BOLD association.

Post-hoc tests were conducted within each significant cluster identified by higher level interactions. This post-hoc analysis was done to facilitate interpretation of complex results.

Percent-signal change values, relative to baseline, were averaged across voxels within each significant cluster for each of the 12 effects of interest for all individual subjects. Using these extracted values in SPSS, repeated-measures ANOVA and post-hoc tests with Bonferroni correction decomposed any individual differences that emerged from the omnibus analysis. Post-hoc tests determined individual differences in activation levels and patterns of response.

Recent evidence demonstrates that traditional methods of implementing fMRI cluster size multiple comparison corrections fail to account for spatial autocorrelations, and thereby do not adequately control for false-positive inferences (Eklund et al., 2016). Therefore, we employed the spatial autocorrelation function (ACF) option when using the AFNI programs 3dFWHMx to estimate intrinsic smoothness in the images and 3dClustSim to estimate the probability of false positive clusters. This option allows for non-Gaussian models and spatial autocorrelation functions and calculates moments of differences to a larger radius (Cox et al., 2017). Clusters were considered significant at a voxel-wise $p < .001$, corrected for multiple comparisons using the spatial autocorrelation function procedures noted above, resulting in a minimum cluster threshold of 57 voxels.

2.7. Examining social reticence differences in brain activity

The main analysis used linear mixed-effects models (3dLME in AFNI) to examine effects of SR on SCR-BOLD relations. The models included SR as a continuous between-subject variable, within-subject factors for attention state (threat appraisal, explicit memory) and morph type (CS-, 20%, 40%, 60%, 80% and CS+), and covaried for number of days between fear conditioning/extinction and extinction recall. For posthoc analyses and illustration purposes we created a high SR group, for children above the median on SR (> .05) and a low SR group, for children below the median (≤ .05) on SR.

2.8. Visit 2 SCR and behavioral data analysis

Effects of threat appraisal and explicit memory conditions on self-report during extinction recall were analyzed using a mixed model regression analysis (SPSS Version 20). Linear and quadratic trends of participant responses to the 6 morphed images—0% (CS+), 20%, 40%, 60%, 80%, and 100% (CS+)—were examined for each task instruction as well as the interaction between linear and quadratic trends and SR group (high SR, low SR). Similar analyses were used to examine SCRs obtained during the extinction recall procedure.

3. Results

3.1. Visit 1 fear conditioning and extinction

The ANOVA for SCR revealed a significant Phase-by-Stimulus interaction, $F(2, 106) = 5.52$, $p = .005$, partial $\eta 2 = .094$. Paired samples t-tests revealed greater SCR response to the CS + relative to the CS- during conditioning, $t(54) = 5.85$, $p < .001$, but not during pre-conditioning or extinction (*ps* > .08). These results indicate successful differential conditioning and extinction for the entire sample, as indexed by SCR. In addition, the main effect of Stimulus was significant, $F(1, 53) = 21.85$, $p < .001$, partial $\eta 2 = .292$. As expected, participants had elevated levels of SCR to the CS+ *vs* CS-. The main effect of Phase was also significant, $F(2, 106) = 5.43$, $p = .006$, partial $\eta 2 = .093$, with elevated SCR responses during conditioning relative to pre-conditioning ($p = .004$). There were no main or interaction effects with SR (*ps* > .35) (Table 2).

3.1.1. Reinforcement learning

We compared SCRs to the CS + and the CS- during the conditioning phase. There was a main effect of Stimulus, such that the SCR responses were stronger to the CS + than to the CS-, $F(1, 54) = 32.01$, $p < .001$. This was qualified by a Stimulus x Trial interaction, such that there was a stronger SCR response to the CS+ relative to the CS- in the early acquisition phase trials, $F(9, 486) = 4.15$, $p < .001$. Thus, the SCR demonstrated rapid conditioning, which then habituated (Fig. 2).

We further characterized the SCRs by fitting a reinforcement learning model. This model characterizes the extent to which the SCR to the CS, trial-by-trial, depends on the previous UCSs. We found a significant learning rate (M = 0.26, SEM = .03, $t(54) = 7.94$, $p < .001$). There was no correlation between the learning rate and SR scores for

Table 2
ANOVA results for Phase-by-Stimuli-by-SR for the two dependent variables.

	Self-report			SCR		
Effect	*d.f.*	*F*	Sig	*d.f.*	*F*	Sig
Effects of Conditioning						
Phase	2, 116	**80.57****	$p < .001$	2, 106	**5.43***	$p = .006$
Stimulus	1, 58	**52.62****	$p < .001$	1, 53	**21.82****	$p < .001$
Phase X Stimulus	2, 116	**22.76****	$p < .001$	2, 106	**5.53***	$p = .007$
Effects of Social Reticence (SR)						
Social Reticence	1, 53	0.20	$p = .658$	1, 48	0.65	$p = .424$
Phase X Social Reticence	2, 106	0.67	$p = .483$	2, 96	0.34	$p = .703$
Stimulus X Social Reticence	1, 53	1.46	$p = .233$	1, 48	0.89	$p = .350$
Phase X Stimulus X SR	2, 106	1.96	$p = .149$	2, 96	0.08	$p = .894$

Note. SCR = Skin Conductance Response; d.f = degrees of freedom. Significant effects are indicated in bold.
* $P < .01$.
** $P < .001$.

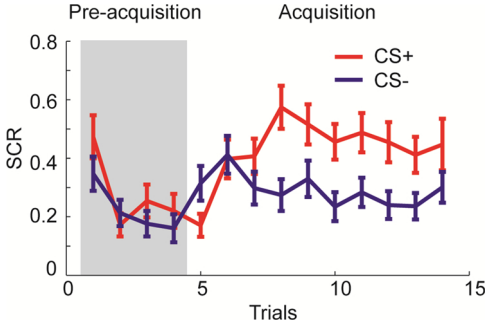

Fig. 2. Trial-by-trial skin conductance response (SCR) to CS+ (red) and CS- (blue) during 4 Pre-acquisition and 10 Acquisition trials. Learning α: M = 0.26, SEM = .03, t(54) = 7.94, p < .001) (For interpretation of the references to colour in this figure legend, the reader is referred to the web version of this article).

individual subjects ($r = -.19$, $p = .78$).

The ANOVA for self-reported fear yielded a significant Phase-by-Stimulus interaction, $F(2, 116) = 22.76$, $p < .001$, partial $\eta 2 = .28$. Paired samples t-tests revealed greater responses to the CS+ *vs* CS- after conditioning and extinction (*ps* < .001). Like SCR, these results indicate successful self-reported differential conditioning for the entire sample; of note, based on subjective report, there was no evidence of successful extinction. In addition, the main effect of Stimulus was significant, $F(1, 58) = 52.62$, $p < .001$, partial $\eta 2 = .48$. As expected, participants reported higher levels of fear to the CS + than the CS-. Finally, the main effect of Phase was also significant, $F(2, 116) = 80.57$, $p < .001$, partial $\eta 2 = .58$. Self-reported fear was higher during conditioning relative to the other two phases (all *ps* < .001). No interaction effects with SR emerged (*ps* > .22).

3.2. Visit 2 extinction recall

3.2.1. Threat appraisal

A linear and a quadratic pattern of self-reported rating were observed for threat appraisal (linear: $B = -0.431$, $SE = 0.103$, $t(125.14) = -4.18$, $p < .001$; quadratic: $B = 0.094$, SE = 0.020, $t(104.69) = 4.66$, $p < .001$). Participants reported more fear the closer stimuli resembled the CS + . Pairwise comparisons revealed greater fear to the CS + than the CS- and compared to each of the other four morphs (all *ps* > .005). That is, participants reported being more afraid of the CS + than the CS- and all GSs. There was no difference in fear rating between the CS- and each of the morphs, indicating youth subjectively experienced equal fear to the CS- and the GSs, but more fear to the CS + . No interaction between SR and morph or SR and morph^2 emerged (all *ps* > .252).

Linear ($B = -0.756$, $SE = 0.296$, $t(168.74) = -2.56$, $p = .011$) and quadratic ($B = -0.431$, $SE = 0.103$, $t(125.14) = -4.18$, $p < .001$) trends were also observed in SCR. In addition, an interaction between SR and morph emerged, with low SR children showing increasing SCR to stimuli resembling the CS+ and high SR children showing elevated SCR to the CS-.

3.2.2. Explicit memory

A linear and a quadratic pattern of self-reported rating were observed for explicit memory (linear: $B = -0.786$, $SE = 0.070$, $t(127.04) = -4.60$, $p < .001$; quadratic: $B = 0.214$, $SE = 0.036$, $t(180.97) = 5.87$, $p < .001$). As with subjective threat appraisal, participants were more likely to report that the bell had rang in the past the more the stimulus resembled the CS+. Significant differences in threat memory were observed between the CS+ and each of the morphs (all *ps* < .001). No interaction between SR and morph or SR and morph^2 emerged (all *ps* > .508). No significant effects were found in explicit memory SCRs (all ps > .462).

3.2.3. fMRI independent of SCR

For the fMRI data, whole-brain random-effects analyses revealed a two-way SR-by-morph interaction in the anterior mid cingulate, thalamus, and middle and superior frontal gyrus (all *ps* > .009). These interactions derived from greater activation to the CS- by high *vs* low SR children in these regions, irrespective of attention state. Two-way attention state-by-morph level interactions in four clusters also emerged: the caudate nucleus ($F = 10.99$, df = 5, 31, $p < 0.001$), thalamus ($F = 10.99$, df = 5, 31, $p < 0.001$), posterior cingulate gyrus ($F = 10.99$, df = 5, 31, $p < 0.001$), and the parahippocampal gyrus ($F = 10.99$, df = 5, 31, $p < 0.001$) (see Table 4 for co-ordinates and voxel-extent). These interactions derived from greater activation to the explicit memory vs. threat appraisal condition at the CS+ ($t(36) = 3.63$, $p < .001$) and 80% morph ($t(36) = 3.58$, $p < .001$) in the caudate nucleus, and the CS+ ($t(36) = 2.54$, $p < .001$) in the posterior cingulate, and parahippocampal gyrus ($t(36) = 2.53$, $p = .016$). For completeness, other brain regions that showed significant two-way interactions in activation during the task are reported in Tables 4 and 5. There were no notable three-way SR-by-attention state-by-morph level interactions.

3.2.4. SCR-BOLD effects

Analysis of brain-behavior covariation focused on the relationship between brain activity and SCRs during extinction recall. Multiple regions showed three-way attention state x morph x SR interactions predicting SCR-BOLD relationships. Fig. 3 present results from the right AIC ($F = 15.45$, df = 5, 25, $p < .0001$), Fig. 4 present results from the right dlPFC ($F = 15.45$, df = 5, 25, $p < .0001$), and Fig. 5 present results from the right aMCC ($F = 15.45$, df = 5, 25, $p < .0001$). These

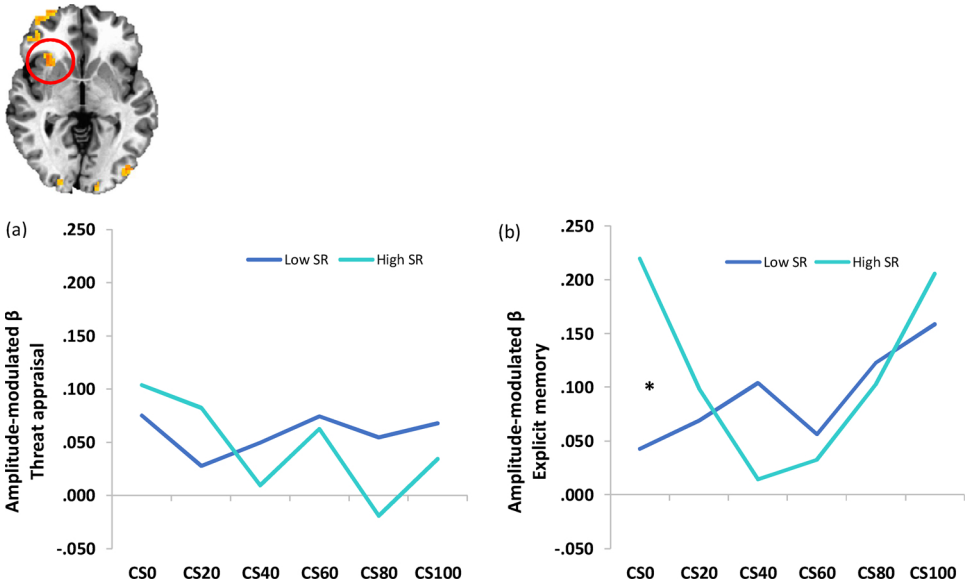

Fig. 3. Social reticence (SR) x Attention State x Morph effects on skin conductance response- blood oxygen-level dependent relationships (amplitude modulation) in the right anterior insula; CS, conditioned stimulus. Peak coordinates, voxel extent, and further information is presented in Table 3.

results are representative of those found in other regions (Table 3). To decompose the three-way interactions, morph x SR interactions were tested for threat appraisal and explicit memory conditions separately. In all three regions, high SR children showed a quadratic relationship between BOLD activity and SCR during the explicit memory condition, while low SR children showed a linear relationship between BOLD activity and SCR. Independent samples t-tests compared high SR to low SR participants for each of the six morph types. The same pattern of results emerged in all three regions: a significant difference at the CS- (rdlPFC: $t(35) = 3.05$, $p = .004$; rAIC: $t(35) = 2.50$, $p = .017$; raMCC: $t(35) = 2.41$, $p = .021$).

4. Discussion

Our data indicate that childhood social reticence predicts a distinct pattern of hemodynamic-autonomic covariation in the brain when recalling extinguished threat and safety cues. Three main findings emerged. First, no effect of SR was detected during fear conditioning or extinction, based on autonomic (SCR) and subjective (self-report) data. Second, during extinction recall, whereas SR influenced children's SCRs during threat appraisal, it did not influence children's subjective behavioral responses to generalization stimuli. Finally, SR exhibited strong associations with brain function, particularly when we examined associations between neural responses and SCR when recalling features of safety cues.

Significant findings are shaped by important negative findings, where no associations with SR manifested. Thus, physiology and self-report data during conditioning revealed that children across all levels of SR learned to differentiate the CS + from the CS-, with effect sizes comparable to previous studies in typically developing children (Gao et al., 2010; Michalska et al., 2016; Pattwell et al., 2012) and children with inhibited and anxious traits (Michalska et al., 2017; Shechner et al., 2015). Consistent with other previous studies (Shechner et al., 2018), we failed to detect associations between SR and either physiology or self-reported fear during extinction learning. While both SCR and self-reported fear demonstrated robust fear conditioning, extinction was observed only in SCR. Again, such findings were expected. Discrepancies between observable fear extinction as measured objectively

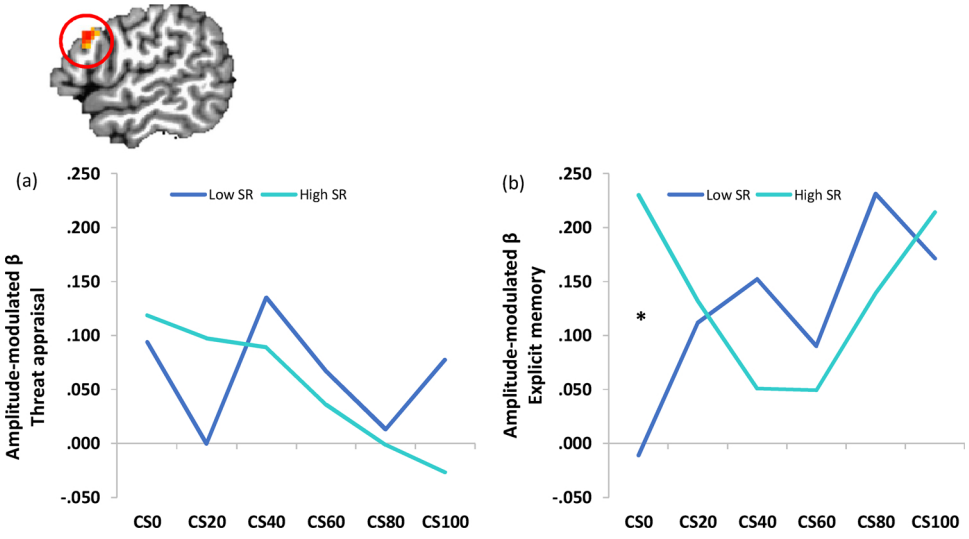

Fig. 4. Social reticence (SR) x Attention State x Morph effects on skin conductance response- blood oxygen-level dependent relationships (amplitude modulation) in right dorsolateral prefrontal cortex (DLPFC); CS, conditioned stimulus. Peak coordinates, voxel extent, and further information is presented in Table 3.

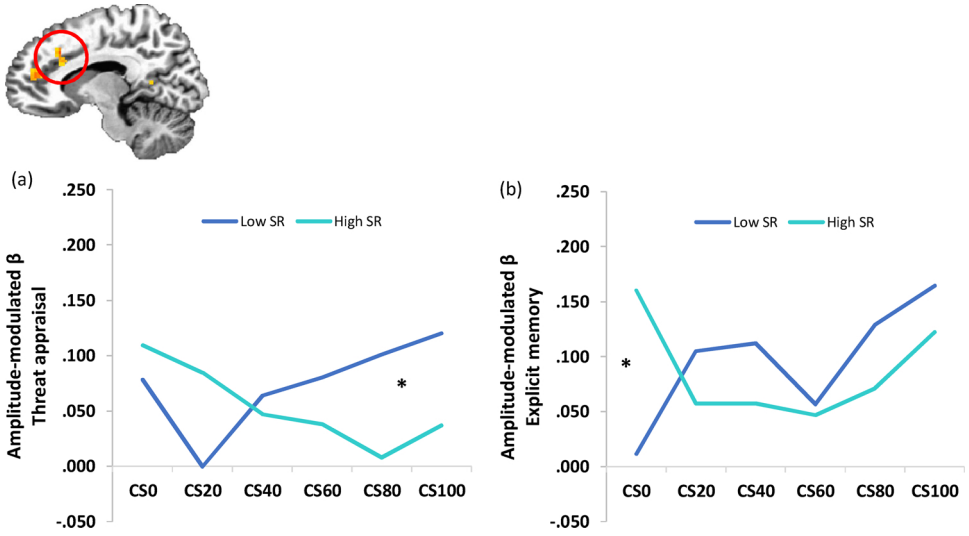

Fig. 5. Social reticence (SR) x Attention State x Morph effects on skin conductance response- blood oxygen-level dependent relationships (amplitude modulation) in right anterior mid cingulate cortex (aMCC); CS, conditioned stimulus. Peak coordinates, voxel extent, and further information is presented in Table 3.

Table 3
Regions of interest that show a three-way association between attention state, social reticence, and morph with SCR-modulated hemodynamic response ($n = 37$, $F = 15.45$, $p < .0001$).

Location	Side	MNI coordinates			Cluster size
		x	*y*	*z*	
Dorsolateral prefrontal cortex	R	54	16	29	204
Superior temporal gyrus/inferior frontal gyrus	L	−36	16	−16	100
Cuneus/middle occipital gyrus	L	−16	−91	11	84
Anterior insula	R	31	21	−1	71
Inferior occipital gyrus/middle occipital gyrus	L	−26	−84	−4	70
Middle frontal gyrus/superior frontal gyrus	R	29	61	−1	66
Supramarginal gyrus/inferior parietal lobule	L	−41	−39	34	57
Anterior cingulate gyrus	R	11	24	34	53
Middle frontal gyrus/inferior frontal gyrus	L	−41	16	24	42
Medial frontal gyrus/anterior cingulate	R	14	41	14	41
Precentral gyrus/middle frontal gyrus	L	−34	−4	41	41
Inferior frontal gyrus	R	46	36	−1	32
Superior temporal gyrus	R	41	11	−24	29
Posterior cingulate	R	21	−46	9	29
Middle frontal gyrus	L	−41	46	19	25

Table 4
Regions of interest that show a two-way association between attention state and morph with hemodynamic response ($n = 37$, $F = 10.99$, $p < .001$).

Location	Side	MNI coordinates			Cluster size
		x	*y*	*z*	
Putamen/caudate	L	−16	9	4	131
Thalamus	L	−19	−16	9	93
Posterior cingulate	L	−9	−29	36	23
Parahippocampal gyrus	R	29	−34	−11	21

(SCR) and subjectively (self-report) have been reported in previous studies that used similar conditioning paradigms in both clinical and nonclinical samples of youth and adults (Britton et al., 2013; Shechner et al., 2015; Waters et al., 2009).

At extinction recall, greater parahippocampal gyrus, posterior cingulate and caudate nucleus activation during the explicit memory compared to the threat appraisal condition was detected across the whole group when the CS + was presented in the context of other generalization stimuli. Previous studies implicate peri-hippocampal structures in the contextual modulation of fear extinction (Kalisch et al., 2006; Milad et al., 2007). Given that the extinction recall component of our task occurred in a context different from the conditioning and extinction contexts (i.e. the fMRI scanner vs. the psychophysiology clinic), the observed activations could reflect attempts by the participants to classify information about contextual cues while recalling extinction. However, further studies with the current paradigm are needed to specifically examine the role of peri-hippocampal structures in context-specific extinction recall, for example by manipulating contextual features of conditioning or adding a renewal test phase.

Greater posterior cingulate cortex activation during explicit recall was detected relative to threat appraisal. Posterior cingulate cortex plays a role in regulating the focus of attention (Hahn et al., 2006), thus ostensibly controlling the balance between internally and externally focused thought. Hence the greater activation within this region in the explicit recall relative to the threat appraisal condition seen in the current study could reflect an effort to monitor fear-relevant stimuli. Significant differences emerged only when an extinguished CS + was presented.

While SR did not relate to self-report data in the current study, individual differences did emerge in neural signatures of long-term retention of fear extinction at extinction recall. Specifically, activity in various cingulate regions increased as a function of temperamental SR. More importantly, associations with SR manifested in analyses that examined SCR-brain activation relationships. In several cortical regions, both SR and attention focus impacted associations between trial-by-trial variation in autonomic responding and brain activation. These interactions occurred in three main brain areas, mainly during explicit recall: the AIC, the aMCC, and the dlPFC. A recent meta-analysis shows that these brain regions are consistently activated during extinction recall studies in adults (Fullana et al., 2018). These results, for an anxiety-related phenotype, resemble prior results on brain-physiology coupling in bipolar disorder and autism (Dalton et al., 2005; Pagliaccio et al., 2017). Across phenotypes, the past and current findings suggest that imaging-based measures of brain activity-physiology coupling, as compared to overall levels of brain activity, are more sensitive to individual differences variables. This could reflect these measures' ability to isolate precise neural correlates of individual difference variables by constraining levels of brain responding based on stimulus-induced,

Table 5
Regions of interest that show a two-way association between social reticence and morph with hemodynamic response ($n = 37$, $F = 10.99$, $p < .001$).

Location	Side	MNI coordinates			Cluster size
		x	*y*	*z*	
Thalamus	L	−1	4	29	627
Cerebellum	L	−36	−64	−39	218
Thalamus	R	6	−26	11	185
Precentral gyrus	R	49	1	26	184
Middle frontal gyrus	L	−36	41	19	89
Middle frontal gyrus	R	36	49	16	73
Superior frontal gyrus	R	6	4	59	71
Precentral gyrus	L	−41	−21	46	68
Caudate	L	−9	19	6	58
Inferior parietal	R	51	−41	49	50
Anterior cingulate	L	−6	41	9	37
Anterior cingulate	L	−1	21	34	28
Inferior frontal gyrus	L	−39	39	1	26
Middle frontal gyrus	R	34	4	46	23
Superior frontal gyrus	L	−16	11	54	20
Superior parietal lobule	R	21	−59	54	20

correlated levels of responding in relevant physiological processes.

Prior research with adults links neural activity in AIC, aMCC, and dlPFC to trial-by-trial variation in SCR, and implicates these regions in the representation of internal bodily states (Critchley et al., 2000, 2001; Fredrickson et al., 1998). In the current study, high SR children showed a quadratic response pattern across morph types, with high SCR-BOLD covariation in the AIC, aMCC and dlPFC when viewing *both* the CS- and CS + . In contrast, low SR children showed a linear pattern of covariation in these regions, increasing from CS- to CS + . Finally, compared to the explicit memory condition, participants' covariation patterns during threat appraisal differed between low and high SR children only in the aMCC, with higher covariation in aMCC for low SR children at the CS + . This is potentially due to the overall low levels of fear evoked at extinction recall, compared to similar paradigms employing social stimuli (i.e. Britton et al., 2013). To explore this possibility, future work should compare the two paradigms directly. Of note, a SR x morph interaction was observed in this condition, whereby high SR children showed elevated SCR to the CS-, compared with low SR children. Even though high SR children did not subjectively report feeling more afraid, their autonomic reaction suggests that they experienced some degree of arousal when viewing this stimulus.

Covariation between activity in the AIC and SCR to the CS + was observed for both high and low SR children. In contrast, when viewing the CS-, such covariation manifested only for high SR children. That is, children with high levels of SR showed a quadratic response pattern across the morph types, whereas children with low SR showed a linear pattern across the morph types. The AIC is thought to be involved in visceral and emotional processing (Phan et al., 2002; Paulus & Stein, 2006), specifically in linking physiological information concerning internal bodily states to goal-related behavior (Carter et al., 1999; Craig, 2009). In the context of the current study, our findings suggest that shy, socially-reticent children have difficulty linking autonomic information to features of a safety cue, such as a CS-. While such difficulty could take many forms, particular features of the current findings provide some clues. For example, children at all levels of SR manifested strong SCR-brain coupling to the CS+, with a gradual decrease for stimuli appearing increasingly dissimilar to the CS + in children with low SR. Children with high levels of SR, in contrast, manifested strong SCR-brain coupling to both the CS + and the CS-. This could reflect momentary re-instantiation of the environment in which these children initially experienced the threatening stimuli. That is, even though the CS- was never paired with the UCS, the CS- (unlike the GS) was present during the conditioning experiment. Thus, children high on SR may be recollecting the situational context in which they experienced both safe and threatening images. It is also possible that high SR children are more confused than low SR children between the two stimuli they encountered in the learning phase. In our previous work (Michalska et al., 2016), we observed that older children (i.e., 9-to-10-year-olds) showed better discrimination and memory than younger children during explicit recall; possibly, highly socially reticent children behave like younger children on this task.

In the aMCC, we also found differences between high-SR and low-SR children in SCR-BOLD coupling to the CSs. The aMCC is reciprocally functionally connected with the AIC (Mesulam and Mufson, 1982). This reciprocity is significant in that their joint activity is thought to be a key component of emotional experience (Carter et al., 1999; Medford and Critchley, 2010). Our finding of covariation between neural responses to fear stimuli in the aMCC and SCR amplitude is consistent with neuroimaging studies in adults. These studies show that activity in the cingulate cortex, spanning pregenual and anterior midcingulate regions, predicts variability in autonomic arousal within individuals and may generate autonomic responses to fearful events (Critchley et al., 2003, 2005; Fredrickson et al., 1998; Milad et al., 2007). However, few studies relate individual differences in SCR-BOLD coupling to real-world behaviors, development, or symptoms. To our knowledge, the current study is the first to demonstrate trial-by-trial covariation between autonomic and central measures in aMCC in preadolescent children and to link them to early social behavior.

Although our data cannot provide evidence for a causal influence of aMCC on SCRs, we propose that at least part of this association could be explained by threat appraisal, which has been related to ACC activity in previous work (Etkin et al., 2011; Maier et al., 2012; Mechias et al., 2010). This proposal is compatible with a recently described neural model of aMCC functional organization. According to this model, the aMCC represents a hub where information about negative emotion and cognitive control are linked to motor centers that guide behavior under conditions characterized by uncertainty of punishment (Shackman et al., 2011). Such uncertainty strengthens the need for cognitive control that would facilitate behaviors intended to facilitate positive outcomes. We found that children high on SR display greater covariation between SCR and aMCC responses to the CS- than children low on SR. This pattern may reflect a mechanism that helps children who are socially reticent reduce the unpredictability of threat and make the correct decision in the face of perceived ambiguity (Alvarez et al., 2011).

A similar pattern of covariation with SCR also emerged in the dlPFC, which is reciprocally connected with the aMCC and likewise involved in strategic control processes (MacDonald et al., 2000; Petrides et al., 1993). PFC activity is associated with several facets of autonomic response to potential threat. Prior research demonstrates that anxiety varies with dlPFC activity during psychological tasks (Basten et al., 2011; Indovina et al., 2011; Wood et al., 2012). Consistent with these observations, we found that covariation between SCR and dlPFC varied as a function of SR. We observed a positive relationship between SCR and SR within this region, such that as SR increased, coupling between the fMRI signal response and SCR to the CS- also increased. Among the key manifestations of SR are fearfulness and restraint in the face of uncertainty (Coplan et al., 1994). Therefore, the observed association between SCR and dlPFC response to the CS- in high SR children may reflect greater cognitive effort needed to not misattribute danger to a safe signal.

4.1. Limitations

The present study addresses the need to integrate central and peripheral approaches to temperament by indexing two specific aspects of biology simultaneously during extinction recall and linking them to early social behavior. Nonetheless, several limitations should be noted. One key limitation is that fMRI responses were only collected at one phase of the experiment. To understand how central and peripheral integration unfold developmentally, future longitudinal imaging studies

will be necessary to elucidate changing patterns of central-autonomic integration and their relation to fear learning. A second limitation is that there were no individual differences in behavioral responding to both conditioned and generalization stimuli. This may be due to the possibility of Type II error but is not entirely unexpected given that lasting effects of temperament are often more evident in brain-behavior associations during an experimental task than in behavioral responses on the task (Bar-Haim et al., 2009; Jarcho et al., 2013, 2016). A third limitation is that behavioral observations were made in the laboratory context only and no concurrent physiological data were acquired; assessments of other childhood phenotypes have used assessments in multiple contexts, and assessments in nonhuman primates have relied on physiology data, acquired contemporaneously with behavior (Fox and Kalin, 2014). Finally, the sample size in the current study was not large. Thus, replication in large samples is needed.

4.2. Strengths

These limitations are offset by several strengths. First, although fMRI data were obtained at only one time-point, participants were assessed on SR based on longitudinal data. Second, scarce work has examined the joint contribution of multiple systems involved in fear learning. Our multimodal approach leads to more refined theories of physiology–brain relations. Finally, studying preadolescents with high childhood SR, yet free of psychiatric impairment, isolates neural correlates associated with risk from neural correlates associated with the expression of psychopathology.

4.3. Conclusions

Childhood temperament strongly predicts a specific aspect of brain function. Specifically, trait social reticence is associated with differences in the coupling between hemodynamic and autonomic response to extinguished threat cues in the brain. Patterns of coupling indicated that adolescents with a history of high SR had selective difficulty tracking safety as a function of how closely the stimulus resembled the safe stimulus. We propose that the study of central–autonomic coupling in emotion promises to generate sophisticated insights into the biological foundations of temperament.

Conflict of interest

The authors declare no conflict of interest related to this work.

Supported by National Institute of Mental Health Intramural Research Program Project number ZIAMH00278, National Institute of Child Health and Human Development (R37HD17899) and National Institute of Mental Health (R01MH093349).

Acknowledgements

This research was supported by the Intramural Research Program of the National Institute of Mental Health (NIMH), Project number ZIAMH00278 National Institutes of Health (NIH).

Appendix A. Supplementary data

Supplementary material related to this article can be found, in the online version, at doi:https://doi.org/10.1016/j.dcn.2018.12.003.

References

Alvarez, R.P., Chen, G., Bodurka, J., Kaplan, R., Grillon, C., 2011. Phasic and sustained fear in humans elicits distinct patterns of brain activity. Neuroimage 55, 389–400. https://doi.org/10.1016/j.neuroimage.2010.11.057.

Balderston, N.L., Helmstetter, F.J., 2010. Conditioning with masked stimuli affects the timecourse of skin conductance responses. Behav. Neurosci. 124, 478–489. https://doi.org/10.1037/a0019927.

Bar-Haim, Y., Fox, N.A., Benson, B., Guyer, A.E., Williams, A., Nelson, E.E., et al., 2009. Neural correlates of reward processing in adolescents with a history of inhibited temperament. Psychol. Sci. 20 (8), 1009–1018.

Basten, U., Stelzel, C., Fiebach, C.J., 2011. Trait anxiety modulates the neural efficiency of inhibitory control. J. Cogn. Neurosci. 23 (10), 3132–3145.

Boucsein, W., 1992. Electrodermal Activity. Plenum Press, New York, NY.

Britton, J.C., Grillon, C., Lissek, S., Norcross, M.A., Szuhany, K.L., Chen, G., Pine, D.S., et al., 2013. Response to learned threat: an fMRI study in adolescent and adult anxiety. Am. J. Psychiatry 170 (10), 1195–1204.

Büchel, C., Morris, J., Dolan, R.J., Friston, K.J., 1998. Brain systems mediating aversive conditioning: an event-related fMRI study. Neuron 20 (5), 947–957.

Carter, C.S., Botvinik, M.M., Cohen, J.D., 1999. The contribution of the anterior cingulate cortex to executive processes in cognition. Rev. Neurosci. 10, 49–57. https://doi.org/10.1093/cercor/2.6.435-a.

Coplan, R.J., Rubin, K.H., Fox, N.A., Calkins, S.D., Stewart, S.L., 1994. Being alone, playing alone, and acting alone: Distinguishing among reticence and passive and active solitude in young children. Child Dev. 65 (1), 129–137.

Costa, V.D., Dal Monte, O., Lucas, D.R., Murray, E.A., Averbeck, B.B., 2016. Amygdala and ventral striatum make distinct contributions to reinforcement learning. Neuron 92 (2), 505–517. https://doi.org/10.1016/j.neuron.2016.09.025.

Cox, R.W., Chen, G., Glen, D.R., Reynolds, R.C., Taylor, P.A., 2017. FMRI clustering in AFNI: false-positive rates redux. Brain Connect. 7 (3), 152–171.

Craig, A.D., 2009. How do you feel–now? The anterior insula and human awareness. Nat. Rev. Neurosci. 10, 59–70. https://doi.org/10.1038/nrn2555.

Critchley, H.D., Elliott, R., Mathias, C.J., Dolan, R.J., 2000. Neural activity relating to generation and representation of galvanic skin conductance responses: a functional magnetic resonance imaging study. J. Neurosci. 20, 3033–3040. https://doi.org/10.1523/jneurosci.20-08-03033.2000.

Critchley, H.D., Harrison, N.A., 2013. Visceral influences on brain and behavior. Neuron 77 (4), 624–638.

Critchley, H.D., Melmed, R.N., Featherstone, E., Mathias, C.J., Dolan, R.J., 2001. Brain activity during biofeedback relaxation: a functional neuroimaging investigation. Brain 124 (5), 1003–1012. https://doi.org/10.1093/brain/124.5.1003.

Critchley, H.D., Mathias, C.J., Josephs, O., O'doherty, J., Zanini, S., Dewar, B.K., et al., 2003. Human cingulate cortex and autonomic control: converging neuroimaging and clinical evidence. Brain 126, 2139–2152. https://doi.org/10.1093/brain/awg216.

Critchley, H.D., Tang, J., Glaser, D., Butterworth, B., Dolan, R.J., 2005. Anterior cingulate activity during error and autonomic response. Neuroimage 27, 885–895. https://doi.org/10.1016/j.neuroimage.2005.05.047.

Critchley, H.D., Nagai, Y., Gray, M.A., Mathias, C.J., 2011. Dissecting axes of autonomic control in humans: insights from neuroimaging. Auton. Neurosci. 161, 34–42. https://doi.org/10.1016/j.autneu.2010.09.005.

Dalton, K.M., Nacewicz, B.M., Johnstone, T., Schaefer, H.S., Gernsbacher, M.A., Goldsmith, H.H., et al., 2005. Gaze fixation and the neural circuitry of face processing in autism. Nat. Neurosci. 8 (4), 519. https://doi.org/10.1038/nn1421.

Dawson, M., Schell, A., Filion, D., 2007. The Electrodermal System. Handbook of Psychophysiology. University Press, Cambridge, MA, pp. 159–181.

Degnan, K.A., Hane, A.A., Henderson, H.A., Moas, O.L., Reeb-Sutherland, B.C., Fox, N.A., 2011. Longitudinal stability of temperamental exuberance and social–emotional outcomes in early childhood. Dev. Psychol. 47 (3), 765. https://doi.org/10.1037/a0021316.

Degnan, K.A., Almas, A.N., Henderson, H.A., Hane, A.A., Walker, O.L., Fox, N.A., 2014. Longitudinal trajectories of social reticence with unfamiliar peers across early childhood. Dev. Psychol. 50, 2311–2323. https://doi.org/10.1037/a0037751.

Eisenbarth, H., Chang, L.J., Wager, T.D., 2016. Multivariate brain prediction of heart rate and skin conductance responses to social threat. Journal of Neuroscience 36 (47), 11987–11998.

Eklund, A., Nichols, T.E., Knutsson, H., 2016. Cluster failure: why fMRI inferences for spatial extent have inflated false-positive rates. Proc. Natl. Acad. Sci 201602413.

Etkin, A., Egner, T., Kalisch, R., 2011. Emotional processing in anterior cingulate and medial prefrontal cortex. Trends Cogn. Sci. 15 (2), 85–93.

Fox, A.S., Kalin, N.H., 2014. A translational neuroscience approach to understanding the development of social anxiety disorder and its pathophysiology. Am. J. Psychiatry 171 (11), 1162–1173. https://doi.org/10.1176/appi.ajp.2014.14040449.

Fullana, M.A., Albajes-Eizagirre, A., Soriano-Mas, C., Vervliet, B., Cardoner, N., Benet, O., et al., 2018. Fear extinction in the human brain: a meta-analysis of fMRI studies in healthy participants. Neurosci. Biobehav. Rev. https://doi.org/10.1016/j.neubiorev.2018.03.002. In Press.

Gao, Y., Raine, A., Venables, P.H., Dawson, M.E., Mednick, S.A., 2010. The development of skin conductance fear conditioning in children from ages 3 to 8 years. Developmental Sci. 13 (1), 201–212.

Goldsmith, H.H., 1996. Studying temperament via construction of the toddler behavior assessment questionnaire. Child Dev. 67 (1), 218–235. https://doi.org/10.1111/j.1467-8624.1996.tb01730.x.

Hahn, B., Ross, T.J., Stein, E.A., 2006. Cingulate activation increases dynamically with response speed under stimulus unpredictability. Cereb. Cortex 17 (7), 1664–1671. https://doi.org/10.1093/cercor/bhl075.

Indovina, I., Robbins, T.W., Núñez-Elizalde, A.O., Dunn, B.D., Bishop, S.J., 2011. Fear-conditioning mechanisms associated with trait vulnerability to anxiety in humans. Neuron 69, 563–571. https://doi.org/10.1016/j.neuron.2010.12.034.

Jarcho, J.M., Davis, M.M., Shechner, T., Degnan, K.A., Henderson, H.A., Stoddard, J., et al., 2016. Early-childhood social reticence predicts brain function in preadolescent youths during distinct forms of peer evaluation. Psychol. Sci. 27, 821–835. https://doi.org/10.1177/0956797616638319.

Jarcho, J.M., Fox, N.A., Pine, D.S., Etkin, A., Leibenluft, E., Shechner, T., Ernst, M., 2013. The neural correlates of emotion-based cognitive control in adults with early

childhood behavioral inhibition. Biol. Psychol. 92 (2), 306–314.
Kaczkurkin, A.N., Burton, P.C., Chazin, S.M., Manbeck, A.B., Espensen-Sturges, T., Cooper, S.E., et al., 2016. Neural substrates of overgeneralized conditioned fear in PTSD. Am. J. Psychiatry 174 (2), 125–134. https://doi.org/10.1176/appi.ajp.2016.15121549.
Kalisch, R., Korenfeld, E., Stephan, K.E., Weiskopf, N., Seymour, B., Dolan, R.J., 2006. Context-dependent human extinction memory is mediated by a ventromedial prefrontal and hippocampal network. J. Neurosci. 26 (37), 9503–9511. https://doi.org/10.1523/JNEUROSCI.2021-06.2006.
Knight, D.C., Nguyen, H.T., Bandettini, P.A., 2005. The role of the human amygdala in the production of conditioned fear responses. Neuroimage 26, 1193–1200. https://doi.org/10.1016/j.neuroimage.2005.03.020.
Kochanska, G., Radke-Yarrow, M., 1992. Inhibition in toddlerhood and the dynamics of the child's interaction with an unfamiliar peer at age five. Child Dev. 63 (2), 325–335.
Li, J., Schiller, D., Schoenbaum, G., Phelps, E.A., Daw, N.D., 2011. Differential roles of human striatum and amygdala in associative learning. Nat. Neurosci. 14 (10), 1250. https://doi.org/10.1038/nn.2904.
Lissek, S., Rabin, S.J., McDowell, D.J., Dvir, S., Bradford, D.E., Geraci, M., Pine, D.S., Grillon, C., 2009. Impaired discriminative fear-conditioning resulting from elevated fear responding to learned safety cues among individuals with panic disorder. Behav. Res. Ther. 47 (2), 111–118. https://doi.org/10.1016/j.brat.2008.10.017.
Lissek, S., Rabin, S., Heller, R.E., Lukenbaugh, D., Geraci, M., Pine, D.S., Grillon, C., 2010. Overgeneralization of conditioned fear as a pathogenic marker of panic disorder. Am. J. Psychiatry 167 (1), 47–55. https://doi.org/10.1176/appi.ajp.2009.09030410.
Lissek, S., Kaczkurkin, A.N., Rabin, S., Geraci, M., Pine, D.S., Grillon, C., 2014. Generalized anxiety disorder is associated with overgeneralization of classically conditioned fear. Biol. Psychiatry 75 (11), 909–915. https://doi.org/10.1016/j.biopsych.2013.07.025.
MacDonald, A.W., Cohen, J.D., Stenger, V.A., Carter, C.S., 2000. Dissociating the role of the dorsolateral prefrontal and anterior cingulate cortex in cognitive control. Science 288 (5472), 1835–1838. https://doi.org/10.1126/science.288.5472.1835.
Maier, S., Szalkowski, A., Kamphausen, S., Perlov, E., Feige, B., Blechert, J., et al., 2012. Clarifying the role of the rostral dmPFC/dACC in fear/anxiety: learning, appraisal or expression? PLoS ONE 7 (11), e50120.
Mechias, M.L., Etkin, A., Kalisch, R., 2010. A meta-analysis of instructed fear studies: implications for conscious appraisals of threat. Neuroimage 49, 1760–1768. https://doi.org/10.1016/j.neuroimage.2009.09.040.
Medford, N., Critchley, H.D., 2010. Conjoint activity of anterior insular and anterior cingulate cortex: awareness and response. Brain Struct. Funct. 214 (5-6), 535–549. https://doi.org/10.1007/s00429-010-0265-x.
Mesulam, M., Mufson, E.J., 1982. Insula of the old world monkey. III: efferent cortical output and comments on function. J. Comp. Neurol. 212, 38–52. https://doi.org/10.1002/cne.902120104.
Michalska, K.J., Shechner, T., Hong, M., Britton, J.C., Leibenluft, E., Pine, D.S., Fox, N.A., 2016. A developmental analysis of threat/safety learning and extinction recall during middle childhood. J. Exp. Child Psychol. 146, 95–105. https://doi.org/10.1016/j.jecp.2016.01.008.
Michalska, K.J., Machlin, L., Moroney, E., Lowet, D.S., Hettema, J.M., Roberson-Nay, R., et al., 2017. Anxiety symptoms and children's eye gaze during fear learning. J. Child Psychol. Psychiatry 58, 1276–1286. https://doi.org/10.1111/jcpp.12749.
Milad, M.R., Wright, C.I., Orr, S.P., Pitman, R.K., Quirk, G.J., Rauch, S.L., 2007. Recall of fear extinction in humans activates the ventromedial prefrontal cortex and hippocampus in concert. Biol. Psychiatry 62 (5), 446–454. https://doi.org/10.1016/j.biopsych.2006.10.011.
Nagai, Y., Critchley, H.D., Featherstone, E., Trimble, M.R., Dolan, R.J., 2004. Activity in ventromedial prefrontal cortex covaries with sympathetic skin conductance level: a physiological account of a "default mode" of brain function. Neuroimage 22, 243–251. https://doi.org/10.1016/j.neuroimage.2004.01.019.
Nieuwenhuis, S., De Geus, E.J., Aston-Jones, G., 2011. The anatomical and functional relationship between the P3 and autonomic components of the orienting response. Psychophysiology 48, 162–175. https://doi.org/10.1111/j.1469-8986.2010.01057.x.
Pagliaccio, D., Wiggins, J.L., Adleman, N.E., Harkins, E., Curhan, A., Towbin, K.E., et al., 2017. Behavioral and neural sustained attention deficits in bipolar disorder and familial risk of bipolar disorder. Biol. Psychiatry 82 (9), 669–678. https://doi.org/10.1016/j.biopsych.2016.09.006.
Pattwell, S.S., Duhoux, S., Hartley, C.A., Johnson, D.C., Jing, D., Elliott, M.D., et al., 2012. Altered fear learning across development in both mouse and human. Proc. Natl. Acad. Sci. 109 (40), 16318–16323.
Paulus, M.P., Stein, M.B., 2006. An insular view of anxiety. Biol. Psychiatry 60 (4), 383–387.
Phan, K.L., Wager, T., Taylor, S.F., Liberzon, I., 2002. Functional neuroanatomy of emotion: a meta-analysis of emotion activation studies in PET and fMRI. Neuroimage 16 (2), 331–348. https://doi.org/10.1006/nimg.2002.1087.
Petrides, M., Alivisatos, B., Meyer, E., Evans, A.C., 1993. Functional activation of the human frontal cortex during the performance of verbal working memory tasks. Proc. Natl. Acad. Sci. 90 (3), 878–882.
Phelps, E.A., O'Connor, K.J., Gatenby, J.C., Gore, J.C., Grillon, C., Davis, M., 2001. Activation of the left amygdala to a cognitive representation of fear. Nat. Neurosci. 4 (4), 437.
Rothbart, M.K., Ahadi, S.A., Hershey, K.L., Fisher, P., 2001. Investigations of temperament at three to seven years: the children's behavior questionnaire. Child Dev. 72, 1394–1408. https://doi.org/10.1111/1467-8624.00355.
Rubin, K.H., Burgess, K.B., 2001. Social Withdrawal and Anxiety. The Developmental Psychopathology of Anxiety. pp. 407–434.
Rubin, K.H., Krasnor, L.R., 1983. Age and gender differences in solutions to hypothetical social problems. J. Appl. Dev. Psychol. 4, 263–275. https://doi.org/10.1016/0193-3973(83)90022-9.
Rubin, K.H., Burgess, K.B., Hastings, P.D., 2002. Stability and social–behavioral consequences of toddlers' inhibited temperament and parenting behaviors. Child Dev. 73, 483–495. https://doi.org/10.1111/1467-8624.00419.
Rubin, K.H., Coplan, R.J., Bowker, J.C., 2009. Social withdrawal in childhood. Annu. Rev. Psychol. 60, 141–171.
Rubin, K.H., Barstead, M.G., Smith, K.A., Bowker, J.C., 2018. Peer relations and the behaviorally inhibited child (In Press) In: Perez-Edgar, K., Fox, N.A. (Eds.), Behavioral Inhibition During Childhood and Adolescence. Springer.
Shackman, A.J., Salomons, T.V., Slagter, H.A., Fox, A.S., Winter, J.J., Davidson, R.J., 2011. The integration of negative affect, pain and cognitive control in the cingulate cortex. Nature Rev. Neurosci. 12 (3), 154.
Shechner, T., Britton, J.C., Ronkin, E.G., Jarcho, J.M., Mash, J.A., Michalska, K.J., et al., 2015. Fear conditioning and extinction in anxious and nonanxious youth and adults: examining a novel developmentally appropriate fear-conditioning task. Depress. Anxiety 32 (4), 277–288.
Shechner, T., Fox, N.A., Mash, J.A., Jarcho, J.M., Chen, G., Leibenluft, E., et al., 2018. Differences in neural response to extinction recall in young adults with or without history of behavioral inhibition. Dev. Psychopathol. 30, 179–189. https://doi.org/10.1017/S0954579417000554.
Stewart, S., Rubin, K.H., 1995. The social problem-solving skills of anxious-withdrawn children. Dev. Psychopathol. 7, 323–336. https://doi.org/10.1017/S0954579400006532.
Tranel, D., Damasio, H., 1994. Neuroanatomical correlates of electrodermal skin conductance responses. Psychophysiology 31 (5), 427–438.
Waters, A.M., Henry, J., Neumann, D.L., 2009. Aversive Pavlovian conditioning in childhood anxiety disorders: Impaired response inhibition and resistance to extinction. J Abnorm Psychol. 118 (2), 311.
Williams, L.M., Barton, M.J., Kemp, A.H., Liddell, B.J., Peduto, A., Gordon, E., Bryant, R.A., 2005. Distinct amygdala?autonomic arousal profiles in response to fear signals in healthy males and females. Neuroimage 28 (3), 618–626.
Williams, L.M., Phillips, M.L., Brammer, M.J., Skerrett, D., Lagopoulos, J., Rennie, C., 2001. et al.. Arousal dissociates amygdala and hippocampal fear responses: evidence from simultaneous fMRI and skin conductance recording. Neuroimage 14 (5), 1070–1079.
Wood, K.H., Ver Hoef, L.W., Knight, D.C., 2012. Neural mechanisms underlying the conditioned diminution of the unconditioned fear response. Neuroimage 60 (1), 787–799.